HARRAN ÜNİVERSİTESİ VETERİNER FAKÜLTESİ DERGİSİ

Geometric morphometric analysis of New Zealand rabbit cranium

Havali AKKAYA[1,a], İftar GÜRBÜZ[2, b, *]

[1] Burdur Mehmet Akif Ersoy University, Institute of Health Sciences Student, Department of Veterinary Anatomy, Burdur, Türkiye.

[2] Burdur Mehmet Akif Ersoy University, Faculty of Veterinary Medicine, Department of Anatomy, Burdur, Türkiye.

[a]ORCİD: 0000-0002-0941-1864;

[b] ORCID: 0000-0001-9460-0645;

Received: 10.11.2023

Accepted: 15.01.2024

How to cite this article: Akkaya H, Gürbüz I. (2024). Geometric morphometric analysis of New Zealand rabbit cranium. Harran Üniversitesi Veteriner Fakültesi Dergisi, 13(1): 14-21. DOI:10.31196/huvfd.1388962.

***Correspondence:** İftar GÜRBÜZ

Burdur Mehmet Akif Ersoy University, Faculty of Veterinary Medicine, Department of Anatomy, Burdur, Türkiye.

e-mail: iftargurbuz@mehmetakif.edu.tr

Available on-line at: https://dergipark.org.tr/tr/pub/huvfd

Abstract: This study, aimed to determine the shape features of the New Zealand rabbit skull and to reveal the differences between individuals and genders in terms of shape features. For this purpose, the geometric morphometry method was used. A total of 10 female and 10 male New Zealand Rabbit craniums were used. The skulls were photographed in a dorsal, ventral and lateral view, and the mandible was photographed in a lateral view. Homologous landmarks were marked on the photographs. Consensus graphs were created by the TpsRelw (Version 1.70) program. Additionally, principal component analysis and relative warp analysis were performed. As a result of the study, principal components explained 34.813%, 57.225% and 42.427% of the total shape difference in the dorsal, ventral and lateral views of the skull, respectively. In the first principal component graph obtained as a result of principal component analysis, no significant clustering was observed between genders. According to the graphics obtained in the MorphoJ program, inter-individual variation was detected mainly in the viscerocranium, followed by the neurocranium. This study will contribute to morphological and archaeological studies on rabbit skulls.

Keywords: Gender, geometric morphometry, mandible, rabbit, skull.

Yeni Zelanda Tavşanı Cranium'unun Geometrik Morfometrik Analizi

Özet: Bu çalışmada Yeni Zelanda tavşanı kafatasının şekilsel özelliklerinin belirlenmesi ve bu özellikler bakımından bireyler arası ve cinsiyetler arası farklılıkların ortaya konulması amaçlandı. Bu amaçla geometrik morfometri yöntemi kullanıldı. Toplamda 10 adet dişi ve 10 adet erkek Yeni Zelanda Tavşanı kafatası kullanıldı. Kafatasları dorsal, ventral ve lateral görünümde, mandibula lateral görünümde fotoğraflandı. Fotoğraflar üzerinde homolog londmarklar işaretlendi. Konsensüs grafikleri TpsRelw (Sürüm 1.70) programı tarafından oluşturuldu. Ayrıca temel bileşen analizi ve relative warp analizi yapıldı. Çalışma sonucunda temel bileşenler, kafatasının dorsal, ventral ve lateral görünümlerindeki toplam şekil farkının sırasıyla %34,813, %57,225 ve %42,427'sini açıklamaktadır. Temel bileşenler analizi sonucunda elde edilen birinci temel bileşenler grafiğinde cinsiyetler arasında anlamlı bir kümelenme gözlenmedi. MorphoJ programında elde edilen grafiklere göre bireyler arası varyasyonun en çok viscerocranium'da, ardından da neurocranium'da olduğu tespit edildi. Bu çalışmanın tavşan kafatasları üzerinde yapılacak morfolojik ve arkeolojik çalışmalara katkı sağlayacağına inanıyoruz.

Anahtar Kelimeler: Cinsiyet, geometrik morfometri, kafatası, mandibula, tavşan.

Introduction

New Zealand White rabbit (Oryctolagus cuniculus L.) belongs to the Craniata group of Chordata, Mammalian class, Lagomorpho order, Laporidae family (McLaughlin and Chiasson, 1979). Rabbits are frequently used in scientific studies because they have a short growth period and are easy to follow before and after the experiment (Mapara et al., 2012). In the rabbit, the skull consists of bones joined by immobile joints. The rabbit's skull has a well-developed posterior section (neurocranium) surrounding the brain and a front section (viscerocranium) consisting of jaws. Orbits are between the posterior section and anterior sections (Farag et al., 2012).

The traditional morphometry method analyzes structure distance and ratios, angle, area and volume measurements statistically (Mitteroecker and Gunz, 2009). The limitations of traditional morphometry analysis methods have led to the emergence of a new method, geometric morphometry, over time (Adams et al., 2004; Aytek, 2017). Geometric morphometry is a method based on the analysis of anatomical points obtained from two- or three-dimensional Cartesian coordinates (Bookstein, 1997; Boz et al., 2023).

There are many geometric morphometric studies on the skull in the literature (Demiraslan et al., 2023; Demircioğlu et al., 2021; Erol and Aytek, 2016; Gündemir et al., 2023; Gürbüz et al., 2020, Gürbüz et al., 2022; Yalçın and Kaya, 2009; Yaprak et al., 2023). However, no study was found in the literature in which the skull and mandible of male and female New Zealand Rabbits were examined using the geometric morphometric method. The aim of the study was to examine New Zealand Rabbit's cranium according to gender using geometric morphometric methods.

Materıals and methods

Ethical approval: Approval for the study was received from Burdur Mehmet Akif Ersoy University Animal Experiments Local Ethics Committee (Date: 13.10.2021, Number: 820).

Materials: A total of 20 adult New Zealand rabbit cranium, 10 female and 10 male, were used in the research. There was no pathology in the craniums. The weights of the male and female rabbits were determined as 1896.72 ± 399.8 kg and 1910 ± 485.9 kg, respectively. After the rabbit cranium was macerated, the skull was photographed in the ventral, dorsal and left lateral directions, and the left mandible was photographed in the lateral direction. These photographs were taken from a distance of 50 cm for all materials.

Geometric morphometric analysis: Photos were saved in JPEG format. Then, a file in Tps format was created with the TpsUtil (Version 1.79) program to place landmarks (LM) on the photographs (Rohlf, 2019). Homologous LMs were ticked on the photographs with the TpsDig2 (Version 2.31) program (Rohlf, 2018). 14 homologous LMs were ticked on the dorsal images of the skulls (Figure 1), 15 on the ventral images (Figure 2), 14 on the lateral images (Figure 3) and 10 on the mandible images (Figure 4). Thus, the Cartesian coordinates of the LMs were determined. Homologous LM validation testing was done with the TpsSmall (Version 1.34) program (Rohlf, 2017). As a result of this analysis, uncentred correlation and root mean square error were specified as 1.000000 and 0.000025 on dorsal images, 1.000000 and 0.000080 on ventral images, 1.000000 and 0.000025 on lateral images, and 1.000000, 0.000033 on mandibles. All these results demonstrated the accuracy of LMs.

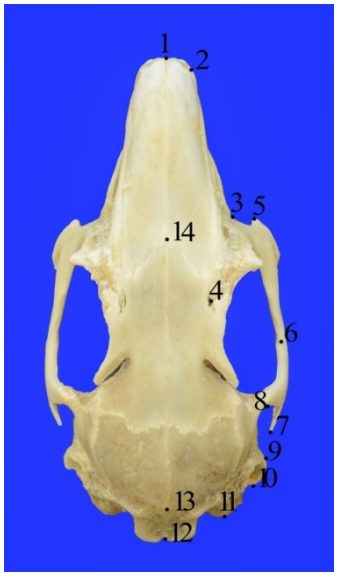

Figure 1. Landmarks on dorsal images of the female skull. **LM1.** Craniomedial of os incicivum, **LM2.** Craniolateral of os nasale, **LM3.** Medial eye angle, **LM4.** Incisura supraorbitalis rostralis, **LM5.** Cranial of arcus zygomaticus, **LM6.** Junction of processus temporalis and processus zygomaticus, **LM7.** Caudal of arcus zygomaticus, **LM8.** Caudomedial of the processus zygomaticus osis temporalis, **LM9.** Cranial external auditory canal, **LM10.** Caudal external auditory canal, **LM11.** Caudal of os occipitale, **LM12.** Caudamedial of the skull, **LM13.** Midpoint of os interparietale, **LM14.** Medial of sutura nasofrontalis.

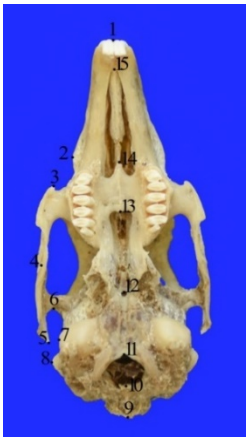

Figure 2. Landmarks on ventral images of a female skull. **LM1.** Craniomedial of os incicivum, **LM2.** Lateral projection of facies facialis, **LM3.** Cranial of tuber faciale, **LM4.** Midpoint of arcus zygomaticus, **LM5.** Caudal of arcus zygomaticus, **LM6.** Caudomedial of the processus zygomaticus osis temporalis, **LM7.** Lateral process of os temporale, **LM8.** Lateral process of the external auditory canal, **LM9.** Caudomedial of os occipitale, **LM10.** Dorsomedial line of foramen magnum, **LM11.** Ventromedial line of foramen magnum, **LM12.** Canalis craniopharyngeus, **LM13.** Caudomedial of os palatium, **LM14.** Craniomedial of the proceussus palatinus of maxilla, **LM15.** Craniomedial of processus palatinus of os incisivum.

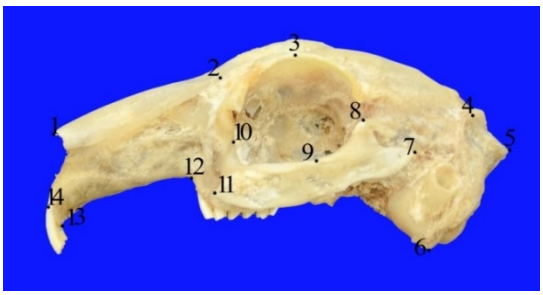

Figure 3. Landmarks on lateral aspect of skull in male rabbit skull. LM1. Craniomedial of os nasale, LM2. Proc of os incivum. caudal of nasalis, LM3. Dorsal of the orbit, LM4. Intersection of os interparietale and os parietale, LM5. Medial of crista nuchae, LM6. Caudoventral of os occipitale, LM7. Caudal of arcus zygomaticus, LM8. Proc. of os temporale. zygomaticus, LM9. Proc of os maxilla. zygomaticus and proc of os temporale. intersection of zygomaticus (midpoint of Arcus zygomaticus), LM10. Medial eye angle, LM11. Cranial end of arcus zygomaticus, LM12. Caudoventral angle of corpus maxilla, LM13. Caudal of the roots of Dentes incisivi, LM4. Craniomedial of os incisivum.

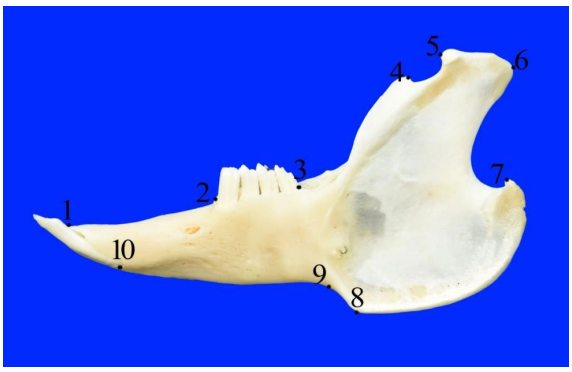

Figure 4. Landmarks identified on lateral views of the mandible in a female New Zealand Rabbit. **LM1**. Craniomedial of os incicivum, **LM2.** Cranial end of premolar tooth root, **LM3.** Caudal of the last molar tooth root, **LM4.** Caudal of proceccus coronoideus, **LM5.** Cranial of processus condylaris, **LM6.** Caudal of processus condylaris, **LM7.** Processus angularis, **LM8.** Cranial end of angulus mandible, **LM9.** Incisura vasorum facialium, **LM10.** Caudal border of incisive tooth root.

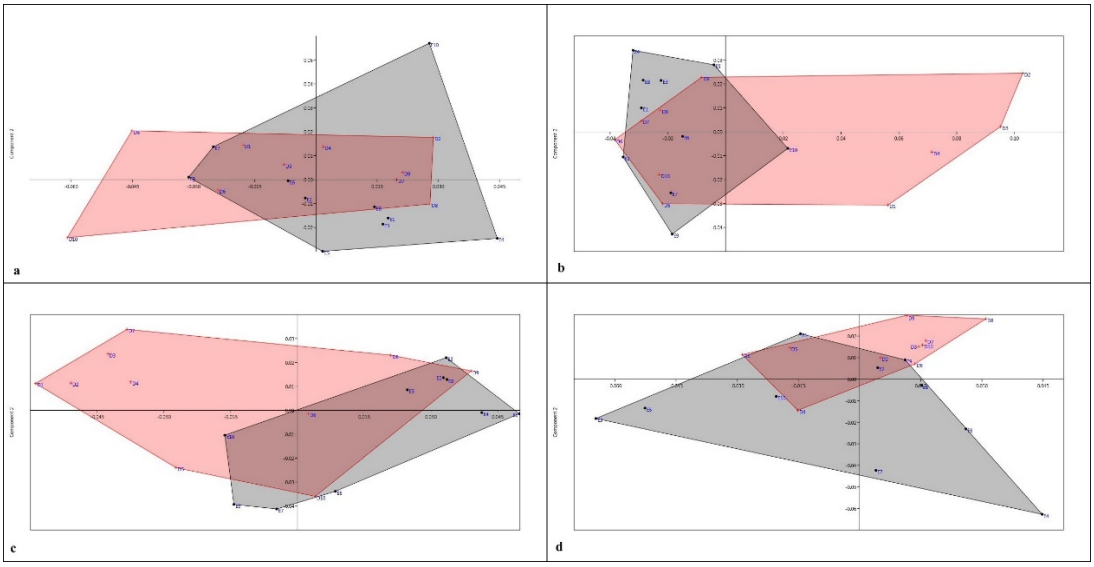

Figure 5. Graphical representation of the results obtained based on the first principal component on skull images. **a**. Dorsal images of skull, **b.** Ventral images of skull, **c**. Lateral images of skull**, d.** Mandible

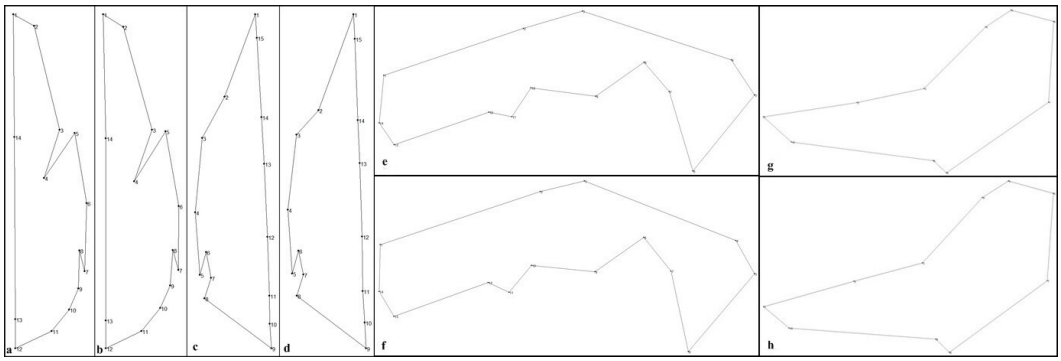

Figure 6. Consensus graph of images of New Zealand rabbit cranium **a.** Dorsal images of female's skull, b. Dorsal images of male's skull, c. Ventral images of female's skull, d. Ventral images of male's skull, e. Lateral images of female's skull, f. Lateral images of male's skull, g. Female's mandible, h. Male'a mandible.

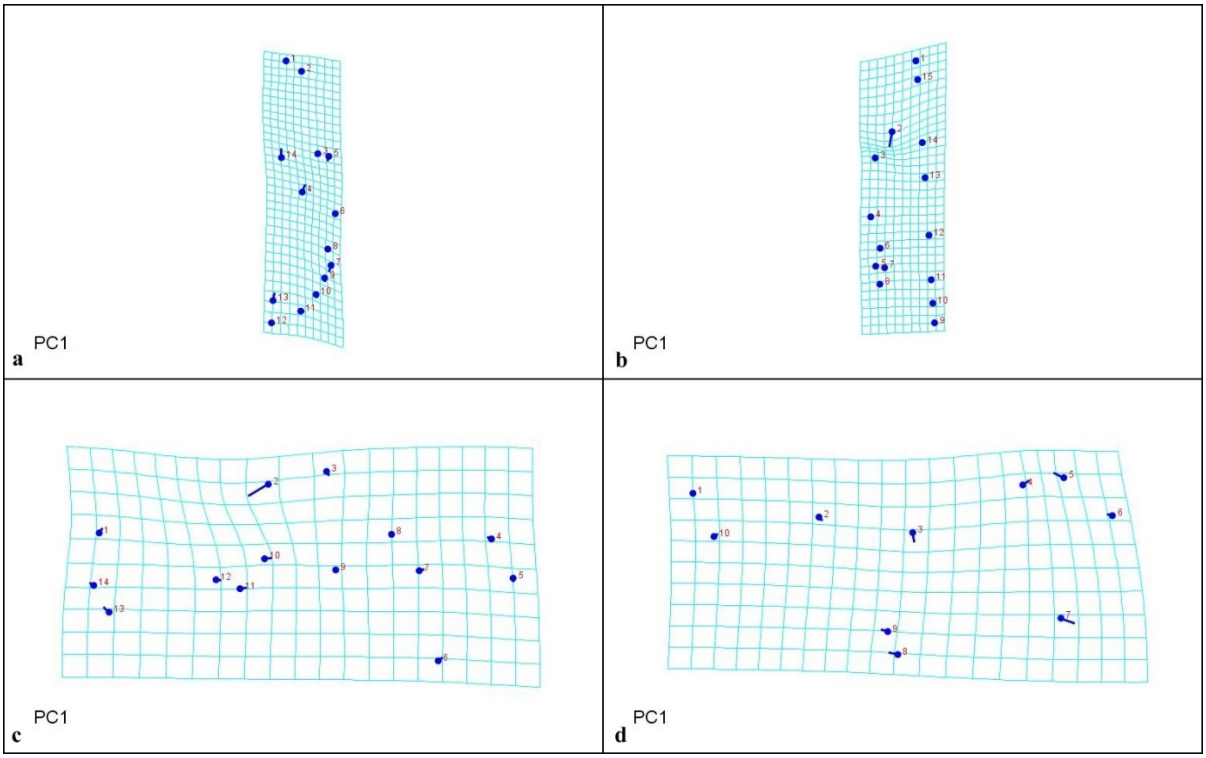

Figure 7. Lollipop graph of PC1 obtained in the MorphoJ program in New Zealand rabbit skull images (Scale factor: 0.05) **a.** Dorsal, **b.** Ventral, **c.** Lateral, **d.** Mandible

In this study, superimposition were applied to the images with Generalized Procrustes analysis (GPA) because the photographs may differ in size, direction and position (Slice, 2007). The PAST (Version 4.02) program was used to perform this analysis (Hammer et al., 2001). After the superimposition was performed, Principal Component (PC) analysis was applied to the new coordinate values that were obtained. Thus, the degree of differentiation of rabbit craniums according to gender was determined. (Zelditch et al., 2004). Additionally, the Morpho J program was used to determine shape differences between individuals. In this program, the differences in LM positions were examined (Klingenberg, 2011). Relative Warp (RW) Analysis was performed in TpsRelw (Version 1.70) program. Consensus graphs of male and female rabbit skulls were created, and the positions of LMs on the figure were determined (Rohlf, 2019). LM coordinate values were compared statistically between genders with the ANOVA test in the PAST (Version 4.02) program.

Results

Table 1 and Table 2 show the results of principal components analysis of the skulls. Accordingly, PC1 explained 34.813%, 57.225% and 42.427% of the total shape differences on dorsal, ventral and lateral views of the skull, respectively. This value was 31.147% on mandible. No significant gender difference according to shape was detected on the images of cranium in PC analysis (Figure 5).

Dorsal images of consensus graphs are shown in Figure 6. No evident difference was observed between groups in consensus graphs. In Relative Warp Analysis, RW1, RW2, and RW3 values in females were determined as %45.51, %19.31, %11.76, respectively. For males, these values were determined as %35.53, %30.45, %10.91, respectively.

Ventral images of consensus graphs were shown in Figure 6 according to gender. The angle at the LM2 (lateral protrusion of facies facialis) in female rabbits was more comprehensive than in male rabbits on ventral images of consensus graphs. In Relative Warp Analysis RW1, RW2, and RW3 values in females were determined as 70.44%, 12.13%, 6.65%, respectively. For males, these values were determined as 39.37%, 32.99%, 10.25%, respectively.

Lateral consensus graphs are shown in Figure 6. According to the consensus graph, it was determined that the distance between the caudal of the processus nasalis of os incisivum (LM2) and the dorsal of the orbita (LM3) in females was larger than in male rabbits. In the Relative Warp analysis, RW1, RW2, and RW3 values were determined as 41.41%, 18.81%, and 12.00% in females, while it was 50.55%, 16.24%, and 13.97% in males, respectively.

The consensus graph of the mandible according to gender is shown in Figure 6. According to Relative Warp analysis, RW1, RW2, and RW3 values in females were determined as 32.96%, 27.19%, and 13.34% while it was calculated as 48.20%, 23.53%, and 17.17% in males, respectively. Accordingly, the mandibles of male rabbits showed more variation in shape.

The lollipop graph of the dorsal images of PC1 is shown in Figure 7 in MorphoJ program. The most significant shape differences on the skull were at the levels of LM14, LM13, LM4, LM7, and LM5, and there was no change in other

Table 1. Values obtained as a result of principal component analysis in dorsal and ventral images of skull.

Dorsal			Ventral		
PC	**Eigenvalue**	**%Variation**	**PC**	**Eigenvalue**	**%Variation**
1	0.000756026	34.813	**1**	0.00198286	57.225
2	0.000400653	18.449	**2**	0.000477659	13.785
3	0.000400653	11.752	**3**	0.000330734	9.5449
4	0.000212493	9.7846	**4**	0.000255298	7.3678
5	0.000151737	6.987	**5**	0.000104652	3.0202
6	0.000125615	5.7842	**6**	7.84149E-05	2.263
7	6.13189E-05	2.8235	**7**	6.15645E-05	1.7767
8	4.85338E-05	2.2348	**8**	5.15237E-05	1.487
9	4.39307E-05	2.0229	**9**	3.59177E-05	1.0366
10	3.12824E-05	1.4405	**10**	2.79973E-05	0.80799
11	2.97296E-05	1.369	**11**	1.72693E-05	0.49839
12	1.48024E-05	0.68161	**12**	1.38285E-05	0.39909
13	1.14935E-05	0.52924	**13**	8.00428E-06	0.231
14	1.04518E-05	0.48127	**14**	6.42042E-06	0.18529
15	7.12679E-06	0.32817	**15**	4.69381E-06	0.13546
16	4.98594E-06	0.22959	**16**	4.14185E-06	0.11953

Table 2. Values obtained as a result of principal component analysis in lateral images of skull and mandible.

Lateral			Mandible		
PC	**Eigenvalue**	**%Variation**	**PC**	**Eigenvalue**	**%Variation**
1	0.00116693	42.427	**1**	0.000737687	31.147
2	0.000535391	19.466	**2**	0.0005561	23.48
3	0.000237603	8.6388	**3**	0.000327111	13.812
4	0.000178557	6.492	**4**	0.000223374	9.4314
5	0.000149407	5.4322	**5**	0.000162846	6.8758
6	0.000111646	4.0592	**6**	0.000103333	4.363
7	0.000102641	3.7318	**7**	8.80964E-05	3.7197
8	7.62102E-05	2.7709	**8**	5.42671E-05	2.2913
9	5.12679E-05	1.864	**9**	4.13815E-05	1.7472
10	3.84636E-05	1.3985	**10**	2.93863E-05	1.2408
11	2.92237E-05	1.0625	**11**	1.90679E-05	0.8051
12	1.84826E-05	0.67199	**12**	9.23555E-06	0.38995
13	1.75771E-05	0.63907	**13**	7.01224E-06	0.29608
14	1.11656E-05	0.40596	**14**	4.97431E-06	0.21003
15	7.94422E-06	0.28884	**15**	2.52123E-06	0.10645
16	6.03891E-06	0.21956	**16**	1.98749E-06	0.083917

Table 3. "p values" in terms of coordinate values of landmarks on images.

Landmark	Dorsal images		Ventral images		Lateral images		Mandible images	
	x coordinate	**y coordinate**	**x coordinate**	**y coordinate**	**x coordinate**	**y coordinate**	**x coordinate**	**y coordinate**
LM1	0.9946	0.5458	0.09037	0.2435	0.006952*	0.7329	0.7757	0.1145
LM2	0.04355*	0.6738	0.0001838*	0.02729*	0.0801	0.01667*	0.1526	0.6855
LM3	0.3778	0.9298	0.1774	0.7697	0.6545	0.8376	0.002772*	0.128
LM4	0.02386*	7.907E-05	0.1673	0.348	0.4977	0.9956	0.0002159*	0.003718*
LM5	0.9743	0.9319	0.3624	0.5166	0.727	0.1354	0.8977	0.9296
LM6	0.5194	0.06281	0.9681	0.3081	0.963	0.5439	0.575	0.8135
LM7	0.5529	0.8109	0.3422	0.3345	0.7748	0.9061	0.003816*	0.8783
LM8	0.339	0.7789	0.6815	0.1238	0.2197	0.9523	0.6027	0.4958
LM9	0.03639*	0.7803	0.3091	0.439	0.09262	0.02086*	0.1166	0.6723
LM10	0.3157	0.5699	0.7505	0.558	0.6758	0.9723	0.9297	0.5214
LM11	0.004593*	0.4387	0.3192	0.2468	0.2884	0.8869		
LM12	0.435	0.9797	0.3919	0.8367	0.6352	0.4245		
LM13	0.4968	0.2872	0.03711*	0.3648	0.5978	0.2724		
LM14	0.1624	0.4372	0.3464	0.02249*	0.2344	0.02622*		
LM15			0.3981	0.003332*				

***: p < 0.05**

landmarks according to PC1. It was seen that LM4, LM13, and LM14 were in the craniodorsal direction, and LM5, LM7 were in the cranioventral direction in the PC1 graph.

The difference in the shape of the skull between individuals was more at the LM2 (lateral protrusion of facies facialis) level on the ventral images in the MorphoJ program. It was determined that LM2 was caudolaterally directed (Figure 7).

On the lateral images, the greatest difference in shape of the skull between individuals was observed at the LM2

level and the LM1, LM3, LM4, LM6, LM7, LM10, LM11, LM12, LM13, and LM14 levels. No shape differences were observed at the LM5, LM8, and LM9 levels in PC1 according to the MorphoJ program (Figure 7).

The lollipop graph obtained according to PC1 on the mandible in the MorphoJ program was shown in Figure 7. It was observed that the shape differences between mandibles were more at the LM5, LM7 levels, and less at the LM3, LM4, LM8, LM9, LM6, LM2 and LM10 levels. In the PC1 graph, it was determined that LM5 was in the craniodorsal direction, LM7 was in the cranioventral direction, and LM8 and LM9 were in the cranial direction. No shape difference was observed at the LM1 level.

Comparison of LMs between genders according to coordinate value and p values are presented in Table 3. A statistically significant difference was determined in some landmarks ($p < 0.05$).

Discussion and Conclusion

In the study, the shape of the New Zealand rabbit skull was determined according to gender using the geometric morphometric method. It was observed that there was no significant separation between male and female rabbits in PC analysis. The highest variation among PCs belonged to the PC1 (57.225%) value determined in ventral images. In the analysis performed in the MorphoJ program, it was observed that the shape difference on the skull mainly was on viscerocranium in the lollipop graphics in PC1 between individuals. In the mandible, the difference in shape was most remarkable in the ramus mandible.

Böhmer and Böhmer, (2017) compared the shape of 12 European rabbit and domestic rabbit skulls and determined high variance in the consensus graph at the level of the craniomedial of the os nasale and the caudal of the os occipitale. In the study, unlike the literature (Böhmer and Böhmer, 2017), it was determined that the most variation was at the LM2 (Lateral view, processus nasalis of incisive bone) level.

Cranial shape is affected by genetic and environmental factors as well as different feeding behaviors (Figueirido et al., 2012). In feeding, chewing muscles determine the direction of movement of the jaw and the chewing force (Gürbüz et al., 2020). Böhmer and Böhmer (2017) stated that the shape difference is mainly in the area where the chewing muscles attach. Chewing muscles that help form mandibular movements and break down food have been examined as masseter, temporal and pterygoideus muscles (Schmolke, 1994; Velasco, 1993). Kabak et al. (2007) reported that the masseter muscles start from the medioventral edge of the maxilla and zygomatic arc, and it connects to the mandibular ramus in the rabbit. The lateral part of the temporal muscles starts from the pars squamosa of the parietal and temporal bone, and it connects to the dorsal end of the coronoid process (Kabak ve ark., 2007). In the study, consistent with the literature (Böhmer and Böhmer, 2017), formal differences were observed in the zygomatic arc and parietal bone, where the chewing muscles are attached. It is thought that the reason for these shape differences between individuals where the chewing muscles are located is due to mandibular movements.

Casanova et al. (2019) used the geometric morphometry method to determine the shape difference between genders in the skulls of wild rabbits (n = 22) and toy rabbits (n = 21). In this study, a difference in skull shape between genders was observed in toy rabbits ($p = 0.034$) and it was stated that this difference was on the splanchnocranium (viscerocranium). Researchers (Casanova et al., 2019) suggested that this difference is because genetic structure affects the change between genders in the developmental process. In this study, consistent with the literature (Casanova et al., 2019), it was observed that the shape differences on lateral images were mostly on viscerocranium.

Casanova and Miquel (2021) examined cranial asymmetry in toy rabbits according to gender. For this purpose, 46 adult (9, male; 37, female) rabbit skulls were photographed from the dorsal aspect and 13 LMs were marked on them. Researchers (Casanova and Miquel, 2021) reported that the shape differences were mostly on the viscerocranium (LM3, LM4, LM13) on dorsal images of the skull. These differences were mostly on the maxilla (cranial of the zygomatic arc) and the lateral protrusions of the nasal bone (Casanova and Miquel, 2021). This study, consistent with the literature (Casanova and Miquel, 2021), it was observed that the shape differences on dorsal images were mostly on viscerocranium. However, unlike the literature, no difference was observed in LM2 determined on the lateral protrusion of the nasal bone on dorsal images. In particular, the difference in the levels of LM14 (medial of the nasofrontal suture) and LM5 (cranial of the zygomatic arc) was evident. Researchers (Casanova and Miquel, 2021) stated that this difference may be related to the growing process.

Although sexual dimorphism varies greatly in populations, the region on the skeleton that best provides gender discrimination is the cranium and pelvis. According to researchers, while gender determination through morphological observations is estimated at 80% using the skull alone, this rate increases to 90% using the skull and mandible together (Güleç et al., 2003; Scheuer, 2002). In the literature, there are some studies on determining sexual dimorphism using geometric morphometric methods on different animal species (Demircioğlu et al., 2021; Duro et al., 2021; Gündemir et al., 2020; Szara et al., 2022).

Gürbüz et al. (2015) examined the differences according to gender in the New Zealand Rabbit skull with the traditional morphometry method. Researchers (Gürbüz et al., 2015) measured 19 different craniometric values in dorsal and ventral aspects of 20 New Zealand Rabbits, 10 males and 10 females. Gürbüz et al. (2015) found the difference between genders statistically insignificant in their study. In the study, no significant gender difference was detected on skull shape images, which is consistent with the literature (Gürbüz et al., 2015).

In conclusion, the shape of the New Zealand rabbit cranium was analyzed using geometric morphometric procedures. According to principal component analysis, male

and female craniums were not concentrated in a particular region in the ventral, dorsal, and lateral images of skull and mandible. Among the principal component analyzes performed in the study, the highest variation belonged to the PC1 (57.225%) determined in the ventral images. As a result of the Relative Warp Analysis, the variation among females (RWA1: 70.44%) was determined most on ventral images, while the variation among males (RWA1: 50.55%) was determined most on lateral images. According to the first principal component on the ventral, dorsal and lateral images, it was observed that the shape difference in the lollipop graphics in the MorphoJ program was higher in the viscerocranium than in the neurocranium. The shape difference in the mandible was on the mandibular ramus. It is thought that the reason for the shape changes in viscerocranium may be due to the difference in chewing function. As a result, we believe that the data obtained will contribute to geometric morphometric studies on the skulls of other rabbit species. It is also essential to provide formal information on the craniums found in zooarchaeological studies.

Acknowledgement

We sincerely thank the Burdur Mehmet Akif Ersoy University Scientific Research Projects -Coordinator (Project number: 0788-YL-21) for supporting of this research work. This study is summarized from the Master Thesis titled “Geometric morphometric analysis of New Zealand Rabbit Cranium” written by Havali AKKAYA.

Conflict of interest

The authors declare that they have no actual, potential or perceived conflicts of interest for this article.

Ethical permission

Permission was received for this study from Burdur Mehmet Akif Ersoy University HADYEK, dated 13.10.2021 and numbered 820. Additionally, the authors declared that Research and Publication Ethics were complied with.

Financial support

This research was supported by Burdur Mehmet Akif Ersoy University Scientific Research Projects Coordination Office (Project no: 0788-YL-21). This study is summarized from the Master's Thesis titled "Geometric Morphometric Analysis of New Zealand Rabbit Skull" written by Havali AKKAYA.

Similarity Rate

We declare that the similarity rate (excluding summary, abstract and references) of the article is 2% as stated in the report uploaded to the system.

Explanation

This study is summarized from the Master Thesis titled as “Geometric morphometric analysis of New Zealand Rabbit cranium” written by Havali AKKAYA. At the same time, this study was presented as an oral/abstract at the "ICAFVP 2nd International Conference on Agriculture, Food, Veterinary and Pharmacy Sciences, 2023".

Author Contributions

Idea/Concept: HA, IG
Design: HA
Supervision/Consultancy: IG
Data Collection and/or Processing: HA, IG
Analysis and/or Comment: HA, IG
Source Search: HA
Writing of the Article: HA, IG
Critical Review: IG

References

Adams DC, Rohlf FJ, Slice DE, 2004: Geometric morphometrics: ten years of progress following the ‘revolution’. *Ital J Zool,* 71, 5-16.

Aytek Aİ, 2017: Geometrik Morfometri. *MASROP E-Dergi,* 11, 1-7.

Bookstein FL, 1997: Morphometric tools for landmark data: Geometry and biology. Cambridge University Press.

Boz İ, Manuta N, Özkan E, Kahvecioğlu O, Pazvant G, Ince N G, Gundemir O, 2023: Geometric morphometry in veterinary anatomy. *Veterinaria*, 72(1), 15-27.

Böhmer C, Böhmer E, 2017: Shape variation in the craniomandibular system and prevalence of dental problems in domestic rabbits: a case study in evolutionary veterinary science. *Vet Sci*, 4(1), 5.

Casanova P, Miquel P, 2021: Diferente Asimetría Craneal Según Sexo en el Conejo Toy. *Int J Morphol*, *39*(3), 864-868.

Casanova P, Pere M, Lloveras L, Nadal J, 2019: Skull sexual dimorphism appears in toy rabbits. *Commun Fac Sci Univ Ankara Series C Biology*, 28(2), 225-231.

Demiraslan Y, Demircioğlu İ, Gürbüz İ, Aksünger Karaavci F, Ortadeveci A, Özgel Ö, 2023: Could there be a relationship between feeding charasteristics and the shape of condylus occipitalis of foramen magnum in mammals? *Turkish J Vet and Anim Sci,* 47, 386 - 486.

Demircioğlu İ, Demiraslan Y, Gürbüz İ, Dayan MO, 2021: Geometric Morphometric Analysis of Skull and Mandible in Awassi Ewe and Ram. *Kafkas Univ Vet Fak Derg,* 27, 43-49.

Duro S, Gündemir O, Sönmez B, Jashari T, Szara T, Pazvant G, Kambo A, 2021: A different perspective on sex dimorphism in the adult Hermann's tortoise: geometric morphometry. *Zool Stud*, *60*.

Erol AS, Aytek Aİ, 2016: Antik Anadolu toplumlarının geometrik morfometrik karşılaştırılmaları. Doctoral dissertation, Antropoloji (Paleoantropoloji) Anabilim Dalı, Ankara Üniv Enstitue of Sosial Science, Ankara/Türkiye.

Farag FM, Daghash SM, Khalifa EFM, Hussein MM, Hagrass S, 2012: Anatomical studies on the skull of the domestic rabbit (Oryctolagus cuniculus) with special reference to the hyoid apparatus. *J Vet Anat*, 5(2), 49-70.

Figueirido B, Serrano AFJ, Palmqvist P, 2012: Geometric morphometrics shows differences and similarities in skull

shape between the red and giant pandas. *J Zool*, 286 (4), 293-302.

Güleç E, Sağır M, İsmail ÖZER, 2003: İnsan İskeletlerinde Foramen Magnum'dan Cinsiyet Tayini. *Ankara Üniv DTCF Derg*, 43(1), 1-9.

Gündemir O, Özkan E, İnce NG, Pazvant G, Demircioğlu İ, Aydoğdu S, Dayan MO, 2020: Investigation of Os Coxae in Horses Using Geometric Morphometry Method. *Harran Üniv Vet Fak Derg,* 9, 170-176.

Gündemir O, Szara T, Eravcı E, Karabağlı M, Mutlu Z, Yılmaz O, Büyükünal SK, Blagojevic M, Parés-Casanova PM, 2023: Examination of Shape Variation of the Skull in British Shorthair Scottish Fold and Van Cats. *Animals*, 13 (614), 1–11.

Gürbüz İ, Aytek A, Demiraslan Y, Onar V, Özgel Ö, 2020: Geometric morphometric analysis of cranium of wolf (Canis lupus) and German shepherd dog (Canis lupus familiaris). *Kafkas Univ Vet Fak Derg,* 26, 525-532.

Gürbüz İ, Demiraslan Y, Aslan K, 2015: Morphometric analysis of the skull of New Zealand rabbit (Oryctolagus cuniculus L.) according to gender. *Arc J Anim Vet Sci*, 1(2), 27-32.

Gürbüz İ, Demiraslan Y, Rajapakse C, Weerakoon DK, Fernando S, Spataru MC, Gündemir O, 2022: Skull of the Asian Paradoxurus Hermaphroditus and the golden Paradoxurus Zeylonensis palm civet Geometric morphometric analysis using palate tooth and frontal landmarks. *Anat Histol Embryol,* 51(6), 718–727.

Hammer Ø, Harper DAT, Ryan PD, 2001: Past: Paleontological statistics software package for education and data analysis. *Palaeontol Electron,* 4(1), 1-9.

Kabak M, Gültiken ME, Onuk B, 2007: Yeni Zelanda tavşanında (Oryctolagus cuniculus L.) articulatio temporomandibularis ve çiğneme kaslarının anatomisi. *Ankara Üniv Vet Fak Derg*, 54(3), 149-15.

Klingenberg CP, 2011: MorphoJ: an integrated software package for geometrik morphometrics. *Mol Ecol Resour*, 11, 353-357.

Kozma C, Macklin W, Cummins LM, Mauer R, 1974: Anatomy, physiology and biochemistry of the rabbit. *The biology of the laboratory rabbit*, 12(1), 55-58.

Kraatz B, Sherratt E, 2016: Evolutionary morphology of the rabbit skull. *PeerJ*, 4, e2453.

Mapara M, Thomas BS, Bhat KM, 2012: Rabbit as an animal model forexperimental research. *Dent Res J,* 9(1), 111-118.

McLaughlın CA, Chıasson RB, 1979: Laboratory Anatomy of the Rabbit. Wm C Brown Publishers, USA.

Mitteroecker P, Gunz P, 2009: Advances in Geometric Morphometrics. *Evol Biol,* 36, 235-247.

Rohlf FJ, 2017: TpsSmall Version 1.34. Ecology & Evolution, SUNY at Stone Brook, USA.

Rohlf FJ, 2018: TpsDig Version 2.31. Ecology & Evolution, SUNY at Stone Brook, USA.

Rohlf FJ, 2019: TpsUtil program Version 1.79. Ecology & Evolution, State University of New York, Stony Brook, NY.

Scheuer L, 2002: Application of Osteology to Forensic Medicine. *Clin Anat*, 15, 297-312.

Schmolke C, 1994: The relationship between the temporomandibular joint capsule, articular disc and jaw muscles. *J Anat,* 184(2), 335.

Slice DE, 2007: Geometrik morphometrics. *Annu Rev Anthropol*, 36, 261-281.

Szara T, Duro S, Gündemir O, Demircioğlu İ, 2022: Sex determination in Japanese Quails (Coturnix japonica) using geometric morphometrics of the skull. *Animals*, 12(3), 302.

Taibo A, 2014: Veterinary Medical Terminology Guide and Workbook. 2nd ed., WILEY.

Velasco JM, Vazquez JR, Collado JJ, 1993: The relationships between the temporomandibular joint disc and related masticatory muscles in humans. *J Maxillofac Surg*, 51 (4), 390-395.

Yalçın H, Kaya MA, 2009: Anadolu yaban koyunu ve Akkaraman koyununun kafa kemikleri üzerinde karşılaştırılmalı geometrik morfometri. *Atatürk Üniv Vet Bil Derg,* 2, 105-116.

Yaprak A, Özgel Ö, Demiraslan Y, 2023: Geometric Morphometric Analysis of Skull in Honamlı, Hair, Kilis and Saanen Goat Using Dorsal Landmarks. *Kocatepe Vet J*, 16(1), 86-92.

Zelditch ML, Swiderski DL, Sheets HD, Fink WL, 2004: Geometric morphometrics for biologists: A primer. *Elsevier Academic Press.*